ISSN 1063-7834, Physics of the Solid State, 2015, Vol. 57, No. 2, pp. 219–228. © Pleiades Publishing, Ltd., 2015.
Original Russian Text © P.V. Kuznetsov, Yu.P. Mironov, A.I. Tolmachev, Yu.S. Bordulev, R.S. Laptev, A.M. Lider, A.V. Korznikov, 2015, published in Fizika Tverdogo Tela, 2015, Vol. 57, No. 2, pp. 209–218.

METALS

Positron Spectroscopy of Defects in Submicrocrystalline Nickel after Low-Temperature Annealing[1]

P. V. Kuznetsov[a, b, *], Yu. P. Mironov[a], A. I. Tolmachev[a], Yu. S. Bordulev[b], R. S. Laptev[b], A. M. Lider[b], and A. V. Korznikov[c]

[a] *Institute of Strength Physics and Materials Science, Siberian Branch of the Russian Academy of Sciences, pr. Akademicheskii 2/4, Tomsk, 634021 Russia*

* *e-mail: kpv@ispms.tsc.ru*

[b] *National Research Tomsk Polytechnic University, pr. Lenina 30, Tomsk, 634050 Russia*

[c] *Institute for Metals Superplasticity Problems, Russian Academy of Sciences, ul. Khalturina 39, Ufa, 450001 Bashkortostan, Russia*

Received June 26, 2014

Abstract—Using the method of measuring the positron lifetime spectra and Doppler broadening annihilation line spectroscopy, the annealing of defects in submicrocrystalline nickel produced by equal channel angular pressing has been studied. In as-prepared samples, the positrons are trapped by dislocation defects and vacancy complexes inside crystallites. The size of vacancy complexes decreases with increasing annealing temperature in the interval $\Delta T = 20–300$°C. However, at $T = 360$°C, the complexes start growing again. The dependence of S-parameter on W-parameter derived from the Doppler broadening spectroscopy has two parts with different inclinations to axes that correspond to different types of primary centers of positron trapping in submicrocrystalline nickel. It has been elucidated that, at recovery stage in the temperature interval $\Delta T = 20–180$°C, the main centers of positron trapping are low-angle boundaries enriched by impurities, while at in situ recrystallization stage in the temperature interval $\Delta T = 180–360$°C, the primary centers of positron trapping are low-angle boundaries.

DOI: 10.1134/S1063783415020225

1. INTRODUCTION

Refinement of material structure to submicron size is known to be a cause for the appearance of specific physical and mechanical properties that are significantly different from those of coarse-grained analogs [1–4]. For instance, submicrocrystalline (SMC) materials have high yield strength and microhardness that in certain cases can be achieved without significant loss of plasticity, which attracts an immediate practical interest [1].

The methods of severe plastic deformation (SPD), particularly the method of equal channel angular pressing (ECAP), are in the range of the most effective methods for producing SMC-materials [1, 5]. During SPD of a material, a part of deformation energy is accumulated as crystal structure defects of various kinds: boundaries of various types, dislocations, vacancies, and their complexes [1, 6–8]. According to [1–8], the most crucial role in the formation of unusual properties of SMC-materials is played by nonequilibrium boundaries of grains that have reduced density, i.e. increased free volume.

The excess energy stored during SPD leads to the metastability of SMC-material structure, which, in turn, results in the rapid localization of deformation and subsequent fracture. To decrease the degree of structure nonequilibrium, the structure is exposed to low-temperature annealing avoiding the significant growth of grains and decrease of mechanical characteristics.

The common features of SMC-material annealing are the relaxation of nonequilibrium defects of the structure, the development of recovery process in crystallites and grain boundaries, recrystallization and grain growth [6]. Furthermore, several kinetic processes with participation of various types of defects develop in the structure of SMC-materials [6–8]. The kinetics of the processes depends on the nature of the material, its purity, degree of accumulated deformation, and method of SPD [1, 6–8]. This causes the scientific interest in the study of the annealing process of SMC-materials produced by SPD-methods. Such interest is related to the investigation of the regularities of relaxation of crystalline structure nonequilibrium state. This also has a practical interest from the point of view of thermal stability of SMC structure and its subsequent deformational behavior [1, 6–8].

The detailed understanding of the role of different defects in the formation of SMC-material properties during the annealing needs the implementation of

[1] The article was translated by the authors.

direct methods that provides high sensitivity and selectivity to a certain type of defects [1, 6–8]. In this regard, the methods of positron spectroscopy [9, 10] are the most effective instruments for studying dislocations, vacancies, and vacancy pores in metals. Recently, such methods have been getting more popular for the investigation of SMC and nanostructured metals [11–14].

The study of positron annihilation in SMC-copper and nickel [11–14] has shown that the positrons are localized in the structure defects that are related with dislocations and complexes of vacancy defects that include several vacancies. The annihilation characteristics of positrons change in several stages in the process of SMC-material annealing, due to the peculiarities of its defect structure formed after SPD.

The aim of the present work is investigation the annealing of defects in SMC-nickel using the method of positron annihilation. The work was performed using the samples, which grain-subgrain structure was studied in papers [15, 16] using scanning tunnel microscopy (STM). Thus, the results of the present work can be directly compared to the results of the works [15, 16].

2. MATERIALS AND METHODS OF INVESTIGATIONS

For the study, we have chosen SMC-nickel with the structure examined in detail in several works [1, 8, 15–18], including the method of positron annihilation [10–13]. The specimen were nickel billets with the purity of 99.998% subjected to equal channel angular pressing (ECAP) along B_c route ($N = 4$ passes) at room temperature which resulted in rectangular blocks with the cross-section of approximately 4×4 mm^2 that were subsequently rolled. The samples were ED-cut across the rolling direction and then mechanically and electrolytically polished. Isochronal annealing of samples was performed at temperatures varying from room temperature to 360°C with the step of 60°C and with the exposure time of 15 min at every temperature. Several samples were subjected to recrystallization annealing at the temperature of 800°C for one hour in argon atmosphere followed by rolling with two reduction rates of $\varepsilon_1 = 7.1 \pm 0.1\%$ and $\varepsilon_2 = 12.0 \pm 0.4\%$.

X-ray diffraction (XRD) analysis of SMC-nickel samples was performed with the use of DRON-7 X-ray diffractometer (NANOTECH Shared Use Center of ISPMS SB RAS) with a CoK_α source, using symmetric reflection scheme without a monochromator. The data was processed using PDWin and POWDER CELL 2.5 software packages. We used the Williamson–Hall analysis for distinguishing the contributions of the size of grain–subgrain structure and microstrains of SMC-nickel into the broadening of a physical profile of lines. The size of coherent scattering regions was obtained by extrapolating the dependence of integral intensity on the value of scattering vector to the zero value of the latter. The microdeformation value was determined by the inclination of the said dependence. The reference sample was a cast annealed pure aluminum A999.

Positron annihilation was studied by positron annihilation lifetime spectroscopy (PALS) and Doppler broadening spectroscopy (DBS). Positron lifetime spectra were measured by a spectrometer described in detail in [19, 20]. The time resolution of the spectrometer is ~240 ps. Spectra of Doppler broadening spectroscopy were measured by a spectrometer based on semiconductor detectors with the resolution of 0.8 and 1.8 keV for the peaks of 122 and 1332 keV, respectively. The detection efficacy was ~20% [21]. The positron source was a ^{44}Ti isotope with the radioactivity of 24.5 μCi. The lifetime spectra and momentum distribution of positron annihilation were measured simultaneously. For every sample we have obtained three positron lifetime spectra having 5×10^6 events in a spectrum. The processing of time spectra was carried out using LT10 software [22, 23].

Doppler broadening spectra with the total statistics of 2.5×10^5 in each spectrum were analyzed using standard SP software package [24].

3. RESULTS

3.1. X-Ray Diffraction Analysis

The XRD analysis of samples showed that the peak intensity of plains (111) in as-prepared SMC-nickel is very small, which testifies the formation of pronounced deformation texture. Annealing of the SMC-nickel samples at $\Delta T = 20$–360°C did not lead to a significant change of the texture. Annealing of the samples at $T \sim 800$°C for one hour causes the formation of annealing texture with the high peak intensity of plains (200).

If the intensity of the peak from plains (200) is 100%, then the relation of intensities for plains (111), (220), and (311) is 0.42 : 0.03 : 0.13, respectively.

During the asymmetric measurement with the turn of the sample for the angle ~5°, the intensity of peak (200) decreases almost three-fold, while the intensity of other peaks stays almost constant. Thus, the XRD analysis data testify that the annealing of SMC-nickel at $T \sim 800$°C for one hour lead to recrystallization and formation of annealing texture with plains (200) oriented in parallel to the plain of the sample's surface.

Figure 1a shows the dependence of the microdeformations in SMC-nickel on the annealing temperature obtained as a result of XRD analysis. Obviously, the annealing at the temperature $T = 60$°C causes increased microdistortions, which agrees with the increased microhardness of such samples in works [15, 16]. The annealing of the samples at $\Delta T = 120$–180°C does not lead to a significant change of the microde-

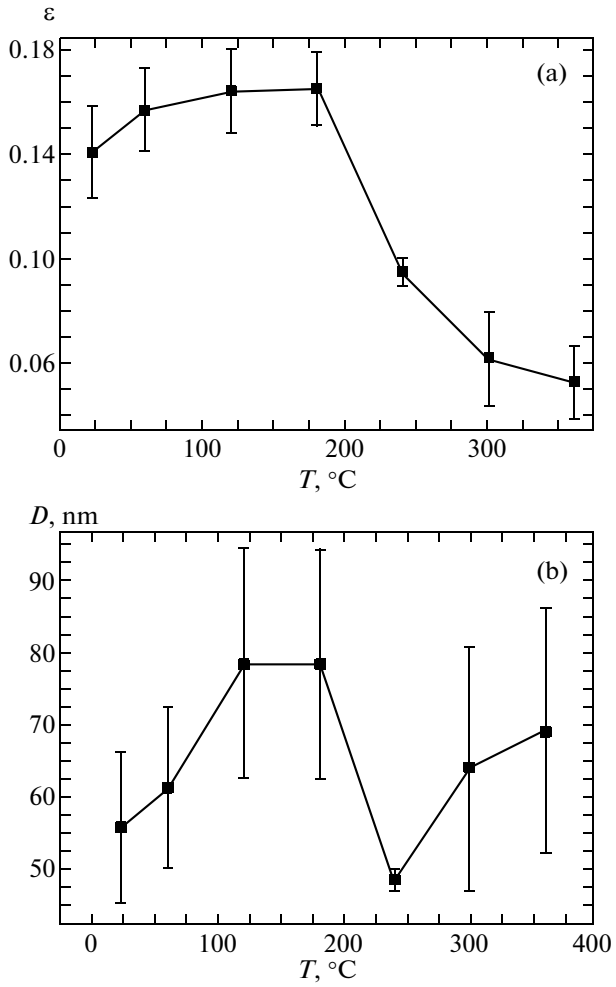

Fig. 1. Dependences of (a) microstrain ε and (b) size of coherent scattering regions in SMC-nickel on the annealing temperature.

formations. The annealing of the samples at the temperature $T \geq 240$°C causes a sharp decrease of microdistortions (Fig. 1a).

The size of coherent scattering regions grow up to ~80 nm at the annealing temperature ranging from room temperature to $T = 180$°C, and then they sharply decrease to ~45 nm after the annealing at $T = 240$°C (Fig. 1b). With a further increase of the annealing temperature, the size of coherent scattering regions increases.

3.2. Doppler Broadening Spectroscopy of Annihilation Gamma-Line

The DBS of annihilation gamma-line allows studying the momentum distribution of electrons [9]. Analysis of spectra of Doppler broadening spectroscopy involves S and W, which are the parameters of a line shape that correspond to annihilation of positrons with outer and inner electrons, respectively. Parameters S and W are the relation of a number of annihilation events in center/wings of distribution plot to the area of the annihilation peak of 511 keV, respectively [9]. Positrons being trapped by vacancy defects, the probability of their annihilation with outer electrons that possess low values of momentum increases, while the probability of annihilation with inner electrons that have high momentum values drops. This leads to increasing the S-parameter and decreasing the W-parameter [9].

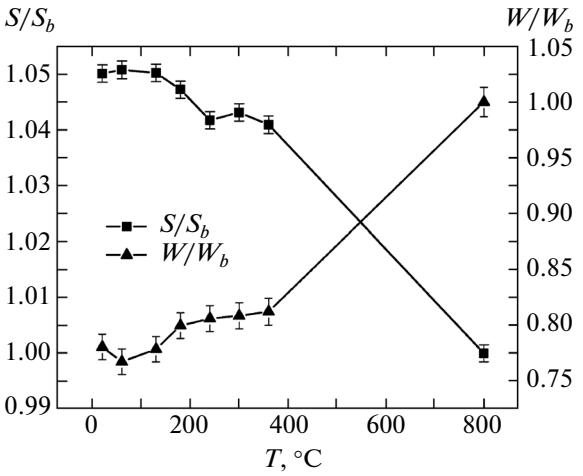

Fig. 2. Dependences of the parameters S and W of the DBS shape on the annealing temperature for SMC-nickel samples. The parameters S and W are normalized to the values of S_b and W_b, respectively, for the recrystallized samples.

Figure 2 show the normalized dependences of S/S_b and W/W_b (where S_b and W_b are values of parameters for recrystallized defect-free samples) on the annealing temperature of SMC-nickel. Evidently (Fig. 2), as-prepared SMC-nickel samples have high values of S-parameter and low values of W-parameter, which corresponds to the positron trapping by vacancy defects. S-parameter does not change within the limits of the experimental error for the temperatures ranging from room temperature to 120°C, and then it sharply decreases in the temperature interval ΔT = 120–240°C. At the annealing temperatures ΔT = 240–360°C the S-parameter remains practically unchanged and reaches its minimum after annealing at $T = 800$°C.

The W-parameter rapidly increases at the annealing temperatures ΔT = 60–180°C and then slightly changes at the temperatures ΔT = 180–360°C and reaches maximal value in recrystallized samples (Fig. 2). Thus, the alteration of the S-parameter with the temperature increase (Fig. 2) testifies the annealing of vacancy defects in the samples of SMC-nickel. We should note that unlike the S-parameter, the W-parameter starts changing at lower annealing temperature of $\Delta T = 20$–180°C (Fig. 2).

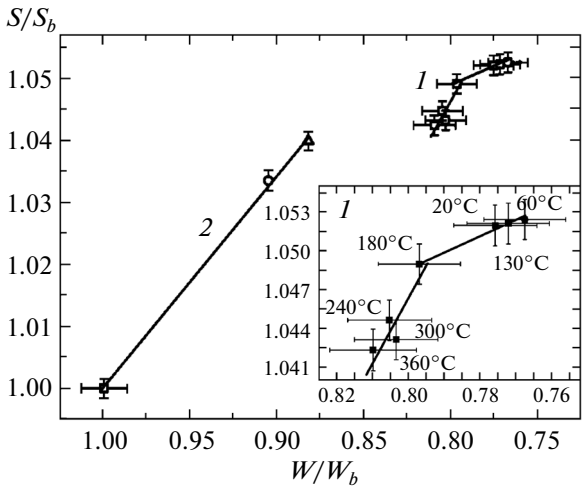

Fig. 3. Dependences of the *S*-parameter on the *W*-parameter: (*1*) as-prepared SMC-nickel samples and samples annealed at different temperatures and (*2*) samples recrystallized and rolled with reduction rates of 7 and 12%.

Both the *S*- and *W*-parameters depend on concentration and type of a defect [9]. The authors of work [25] suggest the parameter $R = (S_d - S_b)/(W_b - W_d)$ that does not depend on the concentration of defects and is determined only by their type, where: S_b, W_b, S_d, and W_d are parameters of DBS shape that are related to positron annihilation in the bulk sample's and (trapped) by defects, respectively. Work [26] suggests a graphical method for analyzing the parameters of DBS shape instead of analytical calculation of the *R*-parameter. According to [26], if the experimental values of the parameters S_d and W_d for the set of samples are in a straight line of a plot $S = f(W)$, this means that the predominant positron traps in the samples are the similar type of defect and which *R*-parameter is determined by the inclination of the straight line. Thus, the change of a straight line S_d, W_d of a plot $S = f(W)$ means the change of *R*-parameter and predominant positron trapping defect. The method [26] can be used in those cases, when all positrons annihilate from the trapping defect states. Implementation of such method does not need the evaluated parameters S_b and W_b.

The top right corner of Fig. 3 show the dependence $S = f(W)$ (indicated by numeral *1*) for as-prepared SMC-nickel and for the samples subjected to annealing in temperature interval $\Delta T = 60$–360°C. The plot is designated by *1*. The inset in Fig. 3 shows the dependence *1* in a larger scale. Figure 3 contains the dependence $S = f(W)$ (curve *2*) for nickel samples recrystallized (denoted by squares) and rolled with two reduction rates of 7 and 12% designated by the circle and triangle, respectively.

As shown in (Fig. 3), the values of *S*- and *W*-parameters of as-prepared and annealed at temperatures of $\Delta T = 60$–360°C samples of SMC-nickel can be represented by two sections of straight lines having different inclinations to axes (dependence *1*). This enables the determination of two *R*-parameter values that correspond to two intervals of annealing temperatures: $\Delta T = 20$–180°C (R_1) and $\Delta T = 180$–360°C (R_2). The obtained result reveals the difference between types of primary positron-trapping defects in the structure of SMC-nickel at the specified temperature intervals.

Values of the *S*- and *W*-parameters for recrystallized and rolled nickel samples can be depicted by a straight line (dependence *2*) with the inclination allowing us to determine the corresponding *R*-parameter.

3.3. Positron Lifetime Spectra

The decomposition of positron lifetime spectra into several exponential components allows obtaining the detailed information on SMC-nickel defect structure after annealing at different temperatures. The presence of components with different characteristic lifetimes of positrons allows identifying the types of defects and evaluating their dimensions and concentration in metals. According to [10], the dislocations and low-angle boundaries provide a typical positron lifetime in metals that is approximately 1.5 times larger than that of positrons in the metal bulk (~108 ps in nickel). Vacancy clusters can provide the positron lifetime that is 1.8–4.1 times larger that of positron in the metal bulk, depending on the number of vacancies [27]. According to [10], the high-angle boundaries of grains can provide a typical positron lifetime of ~2.7 of that of free positrons (~300 ps for copper), which is typical for vacancy clusters. Thus, it is important to bear in mind that various defects in metals can have close values of average positron lifetime [10].

Analysis of positron lifetime spectra in as-prepared SMC-nickel before and after annealing at $\Delta T = 60$–360°C with freely varied parameters enabled the detection of components with specific lifetimes $\tau_1 \sim 108$ ps, $\tau_2 \sim 150$–165 ps, $\tau_v \sim 180$ ps, and $\tau_3 \sim 230$–290 ps. According to [10, 11, 28], the components with $\tau_1 \sim 108$ ps and $\tau_v \sim 180$ ps are related to the annihilation of quasi-free positrons and positrons trapped by monovacancies, respectively. The total intensity of the mentioned components ($I_1 + I_v$) did not exceed 1% for all studied samples. This testifies that the annihilation of positron from quasi-free states and the states conditioned by the presence of monovacancies in the investigated SMC-nickel makes an insignificant contribution. Thus, the positrons in the studied samples primarily annihilate from the states that are localized in the defects having the lifetime $\tau_2 \sim 150$–165 ps and $\tau_3 \sim 230$–290 ps. Dependences of τ_2 and τ_3 and the corresponding intensities I_2 and I_3 on the annealing temperature are depicted in Fig. 4.

Figure 4a shows that the lifetime component τ_2 in as-prepared samples of SMC-nickel after annealing at temperatures of $\Delta T = 60$–240°C is close to 165 ps, which exceeds that of positrons trapped by dislocations in nickel $\tau_{dis} \sim 150$ ps [11]. After annealing at the temperature of $T \geq 300$°C, τ_2 decreases and becomes close to the lifetime of positrons captured by dislocations (Fig. 4a). The intensity I_2 of this component varies from 87% to 95% at $\Delta T = 60$–360°C (Fig. 4b).

The component of positron lifetime $\tau_3 \sim 230$–290 ps testifies the capture of positrons by defects that have larger free volume in comparison to single vacancies and dislocations. The analysis of literature [10, 11, 27] shows that the component τ_3 is related to the annihilation of positrons trapped by vacancy complexes. Using the theoretical dependence of positron lifetime on the size of vacancy complex [28, 30] in nickel, we can evaluate their dimensions in the samples under study. In as-prepared samples of SMC-nickel (Fig. 4a), the component $\tau_3 = 250$ ps corresponds to the annihilation of positrons in vacancy complexes that include up to 5 vacancies [27, 29]. After annealing at the temperature of 60°C, τ_3 reaches its maximum of ~290 ps (Fig. 4a), which corresponds to the size of the vacancy complex with $N = 9$ vacancies. The further increasing of temperature to $T = 300$°C causes the decrease of τ_3 (Fig. 4a), that testify the reduction of the dimensions of vacancy complexes in SMC-nickel to $N = 4$ vacancies [27, 29]. The similar effect of τ_3 decrease accompanying the increase of SMC-nickel annealing temperature was mentioned in the work [11]. We should note that vacancy complexes in the studied samples are not subjected to the annealing up to the temperature of $T = 360$°C. At this temperature, the annealing again initiates the growth of τ_3 (Fig. 4a). Such behavior of τ_3 component of the positron lifetime spectra in SMC-nickel was also noted in [11]. The intensity of I_3 component in the samples under investigation varies from 5% to 14% in the temperature interval $\Delta T = 60$–360°C.

The decomposition with free components of the positron lifetime spectra of recrystallized samples subjected to the rolling with the two reduction rates of $\varepsilon \sim 7.1$ and ~12.6% gives three lifetime components, $\tau_1 \sim 108$ ps, $\tau_2 \sim 148$–160 ps and $\tau_3 \sim 238$–260 ps that correspond to the annihilation of positrons from quasi-free states and localized positrons in defects of dislocation and vacancy types [10, 11, 27]. The intensity of lifetime component of quasi-free positrons (τ_1) after the first rolling was $I_1 = 2\%$, while after the second rolling it reduced to $I_1 = 0.5\%$. Thus, the majority of positrons after the rolling of samples annihilate from the states localized in defects having the typical lifetimes of τ_2 and τ_3.

The lifetime values τ_2, τ_3 and corresponding intensities I_2, I_3 are designated in Figs. 4a and 4b by the indices *1* (7%) and *2* (12%), respectively. The lifetime

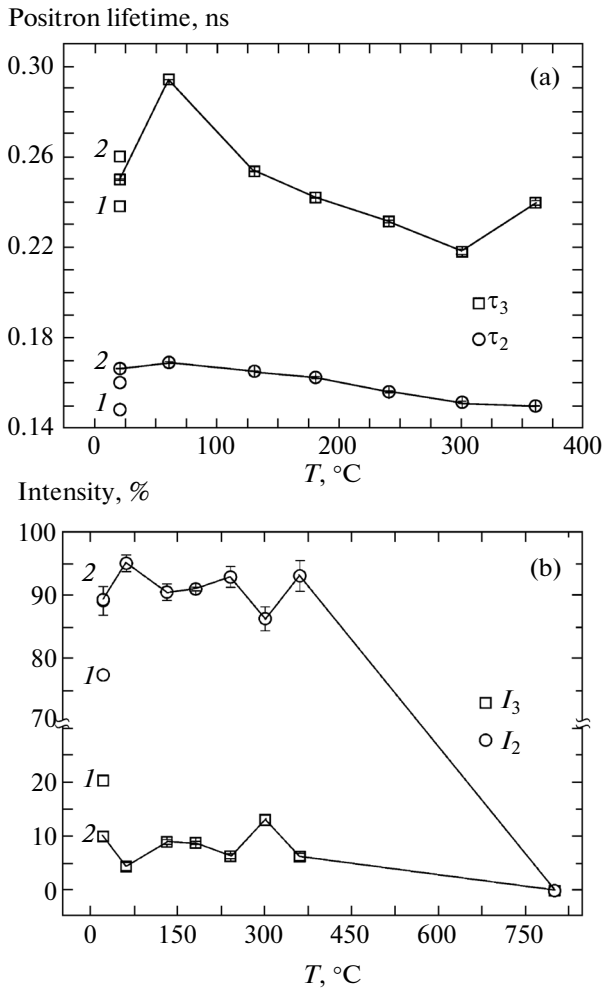

Fig. 4. Dependences of (a) positron lifetime components τ_2 and τ_3 and (b) corresponding intensities I_2 and I_3 on the SMC-nickel annealing temperature The lifetimes τ_2 and τ_3 and corresponding intensities I_2 and I_3 for the recrystallized samples subjected by rolling with two reduction rates $\varepsilon \sim 7.1$ and ~ 12.6% are designated by numerals *1* and *2*, respectively.

of positrons trapped by dislocations τ_2 increases with the growing deformation caused by rolling and approaches to the lifetime of positrons trapped by dislocation defects in SMC-nickel (Fig. 4a). The intensity of I_2 component after the second rolling of samples to the reduction rate $\varepsilon \sim 12.0\%$ is also increased due to the decreased intensity of components I_1 and I_3. It is curious that the positron lifetime $\tau_3 \sim 238$–260 ps in recrystallized and subsequently rolled samples of nickel is close to the component τ_3 of SMC-nickel samples. This evidences that the dimensions of vacancy complexes formed during the rolling of recrystallized samples of nickel are close to those of similar complexes in as-prepared SMC-nickel produced by ECAP method (Fig. 4a).

4. DISCUSSION

Since the majority of positrons in the investigated samples of SMC-nickel annihilate being trapped by defects, their annihilation characteristics contain the information on the peculiarities of the defect structure of studied samples. Accordingly, the discussion of the obtained data should include the results of investigation of defect structure of samples by other methods. The present work is based on the results of the investigation of grain–subgrain structure of the SMC-nickel samples using STM [15, 16] and the data obtained by XRD analysis.

In the works [15, 16] the STM enabled the determination that ECAP and subsequent rolling leads to the formation of nonequilibrium structure in as-prepared samples of SMC-nickel with the average grains size of $\langle d \rangle \sim 200$–$430$ nm across and along the rolling direction, respectively. According to the classification [30], such structure with the average grains size d can be considered as a grain structure containing the dislocation substructure, cells and fragments. By using STM the authors of [15] revealed two processes that develop at two scale levels of grain-subgrain structure of SMC-nickel at the temperatures ranging from 23 to 180°C. At the level of grain assemblies, the authors [15] noted the decrease of the degree of nonequilibrium and reduction of the grains size that reached the minimal dimensions of $\langle d \rangle_{\min} \sim 130$–$170$ nm at $T = 180$°C. The similar effect of grain refinement with the growth of the annealing temperature was detected previously [31] by transmission electron microscopy using the samples of SMC-nickel obtained by the method of hydrostatic pressure torsion (HPT).

At smaller scale [15], we observed the growth of subgrains with the temperature increase reaching the maximum of ~60 nm after annealing at $T = 120$°C. This agrees with the growth of coherent scattering regions measured by XRD analysis (Fig. 1). In the annealing temperature range from 240 to 360°C, using STM, we observed the growth of SMC-nickel grains [15].

Let us consider the issue on the possible centers of positron trapping in the studied samples of SMC-nickel. According to [11], the free path of thermalized positrons in nickel at room temperature is equal to $l_{\text{term}} \sim 150$ nm. Thus, if the average distance between vacancy defects in metal is less than the free path of thermalized positrons, then the positrons will annihilate from the captured-in-defects state.

According to [15], the size of subgrains in the studied samples of SMC-nickel grow within the limits of $\Delta l \sim 35$–60 nm at the annealing temperatures of $\Delta T = 20$–120°C. Accordingly, it is very likely that the main traps of thermalized positrons in the studied samples are low-angle boundaries. With due consideration of the above, let us consider the behavior of annihilation characteristics of positrons in the samples of SMC-nickel during annealing.

As may be inferred from Fig. 2, the S-parameter does not change within the limits of experimental error at the annealing temperature interval $\Delta T = 20$–120°C that, according to [15], is responsible for the decrease of grain size and growth of the size of subgrains. This testifies that S-parameter (being an integral characteristic of excess amount of vacancy defects) turned to be low-sensitive to the rearrangement of low-angle boundaries in the process of the growth of subgrains in such temperature interval.

The better sensitivity in such temperature interval is exhibited by W-parameter (Fig. 2) that is sensitive [9, 32] to a chemical composition in the place of positron annihilation. We can assume that the growth of W-parameter is related to the alteration of chemical composition of low-angle boundaries through the entrainment of impurities from the volume of crystallites in the process of their thermostimulated transportation under strong accumulated strains [15]. Despite the relatively low concentration of impurities in the investigated SMC-nickel, the positrons are able to diffuse easily along the dislocation line until reaching the vacancy defect (e.g., threshold) with the localized impurity. The annihilation of positrons with electrons near the impurity defect is capable of causing the observed changes to W-parameter (Fig. 2).

The decrease of S-parameter in DBS spectra of SMC-nickel samples passes two stages in the temperature interval $\Delta T = 120$–240°C and at $T > 360$°C (Fig. 2). The authors of works [12, 13] have observed the two stages of S-parameter decrease during the annealing of SMC-nickel produced by HPT method (5 revolutions). They supposed that the stage of weak decrease of S-parameter in the temperature interval $\Delta T = 150$–187°C is related to the annealing of vacancies and dislocations. According to [12, 13] the second, more steep stage of S-parameter decrease at the temperature $T > 187$°C is related to the removal of grain boundaries due to recrystallization.

According to [15], at the temperature $T = 180$°C the process of structure refinement is finished and the size of SMC-nickel grains becomes minimal. The dependence $S = f(W)$ (curve *1* in Fig. 3) at the temperature $T = 180$°C show a kink, and it can be represented as two sections that correspond to the following annealing temperature intervals: $\Delta T = 20$–180°C and $\Delta T = 180$–360°C (Fig. 3). The inclination of the section of $S = f(W)$ function in the annealing temperature interval $\Delta T = 20$–180°C (Fig. 3) allows determining parameter R_1 that corresponds to the center of positron capture location and which, according to the above, can be referred to as "impurity enriched low-angle boundaries of grain–subrain structure of SMC-nickel."

Let us consider the second section of $S = f(W)$ function in the annealing temperature interval $\Delta T = 180$–360°C (Fig. 3). The authors of [15] have used STM for observing the increase of SMC-nickel grains

after annealing of the samples at the temperature $T > 240$°C. The results of XRD analysis show (Fig. 1a) that after annealing the samples at the temperature $T >$ 240°C there is a decrease of microdeformations. These results unambiguously testify the initiation of SMC-nickel structure recrystallization.

The XRD analysis of the samples also showed that the SMC-nickel deformation texture is retained after annealing in the temperature interval $\Delta T = 20-360$°C. Thus, the recrystallization of SMC-nickel at $T >$ 240°C is not related to the occurrence of grains with another orientation.

There are different mechanisms of SMC-nickel grain growth with the preservation of a texture during sample heating. The data [1, 6] show that in SMC material obtained by SPD methods so-called anomalous growth of grains conditioned by the growth of certain grains (more weakly deformed) at the expense of other grains (more severely deformed) can occur. The driving force of this process is a local nonuniformity of dislocation density at both sides of the boundary conditioned by the nonuniformity of a deformation. In this case, certain grains grow to the size several times exceeding the average size of material's grains. Such growth is due to the moving of high-angle boundaries. The volumetric fraction of such grains increases exponentially depending on time [1, 6].

On the other hand, the growth of grains can occur due to so-called "in situ recrystallization" or, according to another terminology, collective polygonization [6]. The driving force of such process is the decreasing energy of the system due to the contraction of span of low-angle boundaries resulted from the growth of larger subgrains at the expense of lesser ones. Consequently, the system energy decreases by the value of the energy of low-angle boundary that separates subgrains. In this case, the average misorientation angle between the subgrains does not increase and the subboundaries preserve low-angle characteristics [6]. During the in-situ recrystallization the deformation texture does not change. Work [1] noted the possibility of such scheme of SMC-nickel structure evolution during the annealing process.

Certain interesting details of SMC-nickel microstructure annealing were observed by the authors of [33]. This work covered the study of samples obtained by ECAP method via B_{c4} route. The structure of as-prepared SMC-nickel samples shows numerous deformation bands with the average size of grains of ~250 nm. We observed similar deformation bands at the surface of SMC-nickel samples examined by STM [16]. The annealing of samples at high temperature $T = 700$ K for 17 h lead in [33] to nonuniform recrystallization and growth of grains. The authors of [33] discovered an interesting effect: small grains should have been more severely deformed and, hence, be more susceptible to the growth of grains and recrystallization; however, against expectation, the small grains show greater resistance to recrystallization, contrary to the expressed growth of grains in surrounding regions [33]. The work [33] showed that the cause of such stability of small grains is specific structure elements that contain rotational defects with the misorientation gradient of 10 deg/μm along the band direction and, hence, perpendicular to the boundaries of high-angle interfaces. Authors of [33] assume that since the growth of bended grains causes the increase of crystal energy, then this growth is prohibited until the rotational defect is eliminated. On the contrary, the elements constrained by low-angle boundaries of ~5° show the tendency to coarsening due to the movement of their boundaries and assimilation of neighboring grains. Special studies show that the deformation texture does not change after annealing the samples at the temperature of 750 K for 17 h. Taking into account all the above, we assume that the growth of grain size in our SMC-nickel samples at $T > 240$°C is conditioned by the movement of low-angle boundaries.

Additional information that facilitates understanding the nature of defects that capture positrons corresponding to the second section of $S = f(W)$ dependence in the annealing temperature interval $\Delta T =$ 180–360°C was obtained from the analysis of data for recrystallized and rolled nickel samples (Fig. 3).

Figure 3 shows that the inclination of curve *1* of $S = f(W)$ function in the annealing temperature interval $\Delta T =$ 180–360°C for as-prepared and annealed SMC-nickel samples is close to the corresponding value for recrystallized and rolled nickel samples (curve *2*). This can mean that the nature of defects the main positron traps in these two cases is similar.

The dislocations are known [9] to be the main centers of positron trapping during the moderate plastic deformation of metals. This is the reason why R-parameter that is determined by the inclination of curve *2* of function $S = f(W)$ for recrystallized and rolled nickel samples (Fig. 3) can be associated with dislocations.

With a due account of the aforesaid, the second section of dependence *1* in the annealing temperature interval $\Delta T =$ 180–360°C, which is characterized by R_2-parameter (Fig. 3) can be associated with the prevailing center of positron trapping in SMC-nickel, i.e., low-angle boundaries.

The results of measurements of positron lifetime spectra of studied samples do not contradict the proposed interpretation of the results of measurement of the DBS spectra.

It is known [10] the positron lifetime spectra are sensitive mainly to changes in the free volume. Unlike the positron lifetime spectra, the DBS spectra may reflect changes in the chemical environment at the site of positron annihilation [9, 32]. Therefore positron lifetime characteristics of the investigated samples do not revealed any annealing step associated with the restructuring of small-angle boundaries due to

changes in their chemical composition in the temperature range $T = 20–180°C$ (Fig. 4).

In our work, the behavior of components of positron lifetime spectra of SMC-nickel in dependence on the annealing temperature reveals both common features and differences with the results obtained by the authors of work [11]. The common feature are that in both cases in as-prepared SMC-nickel samples the positrons annihilate from the states associated with the defects of two following types: dislocation defects and vacancy complexes that correspond to the components of positron lifetime spectra τ_2 and τ_3. The difference in the behavior of positron lifetime spectra depending on the annealing temperature testified the significant difference in the defect structure of SMC-nickel samples studied in our work and in work [11].

At the annealing temperature $T > 220°C$, the authors of [11] observed the appearance of a new component of positron lifetime $\tau_1 \sim 100$ ps the intensity of which increases with increasing annealing temperature. We did not detect similar effect in the positron lifetime spectra of investigated SMC-nickel samples.

The SPD method is known to have a significant influence on the features of obtained SMC structure of metals. The samples of SMC-nickel studied in [11] were produced by HPT method with the total logarithm deformation $\varepsilon = 7$. According to [1, 6], the implementation of HPT method causes the formation of more fine-grained and uniform structure in comparison to ECAP method with the same number of passes. The average grain size in [11] was about 114 nm. According to [11], the internal volumes of grains, being almost free of dislocations, are divided by the regions of severely deformed material having greater density of dislocations. The authors of [11] used transmission electron microscopy to show that the misorientations in the regions of severely deformed material are high-angle, and they are characterized by strong nonequilibrium. We should note that high-angle misorientations indicate that the deformation structure of samples has high excessive density of dislocations of like sign, which is a necessary criterion for the formation of recrystallization nuclei and growth of new grains [6].

The SMC structure of the samples studied in our work was obtained by ECAP method after four passes with the total accumulated deformation $\varepsilon \sim 4$. Therefore, in the structure of such samples, the fraction of high-angle boundaries is significantly less; it includes larger grains that contain substantial amount of dislocations and low-angle boundaries. Such structure turns to be less prepared to the beginning of the recrystallization. For this reason, the initial stage of the low-temperature annealing of our samples includes the recovery, the refinement of the structure, the formation of high-angle boundaries and the preparation of conditions for recrystallization. This causes the difference between the positron lifetime spectra of our samples and the data obtained in [11].

The positron lifetime spectra component $\tau_2 \sim 165$ ps in our samples (Fig. 4a) apparently is a superposition of positron annihilation contributions into various defects with close positron lifetimes. Such defects can be low-angle boundaries, dislocations and vacancies. If the concentration of vacancies is less than the threshold sensitivity of electron-positron annihilation method, then component $\tau_v \sim 180$ ps associated with the capture of positrons by vacancies will not be resolved in positron lifetime spectra, but it will make a contribution into τ_2 leading to the increase of its value. The vacancies in nickel become movable at the temperature $T > 100°C$ [11]. This result in the annealing of the vacancies at the temperature $T > 120°C$, which leads to the decrease of their relative contribution into τ_2 and to the reduction of this component (Fig. 4a).

The positron lifetime $\tau_3 \sim 250$ ps in as-prepared SMC-nickel samples is substantially less than the positron lifetime in high-angle boundaries that according to [8] equals to $\tau_b \sim 2.7\tau_f = 290$ ps. Furthermore, the behavior of component τ_3 in relation to the increase of annealing temperature described in our work and in [11] does not allow correlating it with the annihilation of positrons captured by high-angle grain boundaries. Therefore, we along with the authors of [11] associate the component τ_3 with the annihilation of positrons captured by vacancy complexes. The corresponding sizes of vacancy complexes equal to $D \sim 5$ vacancies in our samples and to $D \sim 11–12$ vacancies in samples studied in [11]. Obviously, the dimensions of vacancy complexes are related to the value of plastic deformation ε accumulated during the development of SMC-structure in nickel. Since $\varepsilon = 7$ in work [11] and $\varepsilon = 4$ in our study, the sizes of vacancy complexes in work [11] are greater than the size of similar defects in the samples investigated in our work.

With increase of annealing temperature, the sizes of vacancy complexes in the studied samples decrease (Fig. 4a) similarly to work [11]. The decrease of τ_3 in [11] begins at $T > 160°C$, while in our study it begins at $T > 60°C$. The authors of [11] explain the observed effect of anomalous growth of grains that initiates at the temperature $T \sim 160°C$ and leads to the entrainment of a part of vacancy complexes by a moving recrystallization front. The decrease of vacancy complex size in our samples can occur due to their entrainment by low-angle boundaries during the growth of subgrains at the temperatures from 60 to 300°C (Fig. 4) [17]. However, the vacancy complexes in SMC-nickel show a high stability even after the annealing; for instance, at $T = 360°C$ they start to grow again. The similar effect was discovered by the authors of [11].

We should point out that the ratios of the intensities $I_2 \sim 90\%$ and $I_3 \sim 10\%$ in as-prepared samples deter-

mined in our study and in work [11] are very close. Apparently, this evidences that the mechanism of vacancy complex formation and their spatial distribution inside crystallites is determined by peculiarities of crystalline nickel structure and does not depend on SPD method used for developing the SMC-state. This is also evidenced the formation of vacancy complexes in rolling recrystallized samples, which is detected by measuring the lifetime spectra of positrons (Fig. 4a).

This may be due to the fact that certain configuration of trivacancies and tetravacancies are more energetically favorable than the rest types of vacancy defects. This confirmed the results of investigation of vacancy cluster stability using computer-aided modeling by minimization of total displacement energy of atoms interacting through pairwise potentials [34]. In particular, the close-packed trivacancy can relax into the configuration consisting of a regular tetrahedron containing four vacancies with an internode atom in its center [34].

Authors of works [35, 36] established that the nanopores formed in the process of ECAP have a significant effect on the properties of SMC materials, while a certain level of nanoporosity is capable of evening the hardening process stipulated by ultrafine-grained structure. The high stability of vacancy clusters in SMC-nickel that was observed in the present work and in [11] attests to the conclusions made in [35, 36] and allows explaining the low efficacy of low-temperature annealing that was performed in [15, 16] for the purpose of increased plasticity of samples. Apparently, the vacancy complexes are the nucleation centers for nanopores that in turn can lead to the origination of microcracks, their development of destruction of samples during plastic deformation.

5. CONCLUSIONS

The analysis of the study of annihilation characteristics of positrons and XRD analysis data of SMC-nickel samples considering the results of STM investigation of the evolution of their grain-subgrain structure after low-temperature annealing presented in [15, 16] allow drawing the following conclusions:

(1) In as-prepared SMC-nickel samples, the positrons are captured by dislocation-type defects and vacancy clusters that can include several vacancies.

(2) The change of S- and W-parameters of DBS spectra indicates the annealing of vacancy defects and the alteration of their nearest chemical environment with the growth of SMC-nickel annealing temperature.

(3) The dependence of W-parameter on S-parameter has two inclined regions for the following temperature intervals: $\Delta T = 20–180$°C and $\Delta T = 180–360$°C, which corresponds to two values of R-parameters (R_1, R_2) and two predominant types of defects, positron traps.

(4) The predominant centers of positron capturing in the temperature interval $\Delta T = 20–180$°C that correspond to R_1-parameter are low-angle boundaries that in the process of their own movement entrainment the impurities contained in crystallites.

(5) The recrystallization and growth of grains during SMC-nickel sample annealing at $T > 240$°C occurs due to the collective polygonization (in-situ recrystallization) via the movement of low-angle boundaries, which preserves the deformation texture and leads to decreased microdistortions measured by XRD analysis. Hence, the low-angle boundaries can be assumed to be the predominant centers of positron capturing that correspond to R_2-parameter in the annealing temperature interval $\Delta T = 180–360$°C.

(6) The vacancy complexes show a high stability in SMC-nickel structure. The growth of annealing temperature leads to the decrease of their dimensions due to the partial entrainment of complexes by moving low-angle boundaries; however the vacancy complexes are not completely annealed, and after the annealing at $T = 360$°C they begin to grow again.

ACKNOWLEDGMENTS

This study was supported by the Siberian Branch of the Russian Academy of Sciences (project no. III.23.1.1), the Council on Grants from the President of the Russian Federation for Support of Leading Scientific Schools (grant no. NSh-2817.2014.1), and the Program of Increase in Competitiveness of the National Research Tomsk Polytechnic University.

REFERENCES

1. R. Z. Valiev and I. V. Aleksandrov, *Nanostructured Materials Produced by Severe Plastic Deformation* (Logos, Moscow, 2000) [in Russian].
2. R. A. Andrievskii and A. M. Glezer, Phys.—Usp. **52** (4), 315 (2009).
3. H. Gleiter, Prog. Mater. Sci. **33**, 223 (1989).
4. M. Lu, L. Dao, R. J. Asaro, J. T. M. De Hosson, and E. Ma, Acta Mater. **55**, 4041 (2007).
5. V. M. Segal, V. N. Reznikov, V. I. Kopylov, D. A. Pavlik, and V. F. Malyshev (Navuka i Tekhnika, Minsk, 1994) [in Russian].
6. S. S. Gorelik, S. V. Dobatkin, and L. M. Kaputkina, *Recrystallization of Metals and Alloys* (Moscow Institute of Steel and Alloys, Moscow, 2005) [in Russian].
7. T. Knudsen, W. Q. Gao, A. Godfrey, Q. Liu, and N. Hansen, Metall. Mater. Trans. A **39**, 430 (2008).
8. A. P. Zhilyaev and A. I. Pshenichnyuk, *Superplasticity and Grain Boundaries in Ultrafine-Grained Materials* (FIZMATLIT, Moscow, 2008) [in Russian].
9. R. Krause-Rehberg and H. S. Leipner, *Positron Annihilation in Semiconductors: Defect Studies* (Springer-Verlag, Berlin, 1999).
10. T. E. M. Staab, R. Krause-Rehberg, and B. Kieback, J. Mater. Sci. **34**, 3833 (1999).

11. J. Cizek, I. Prochazka, M. Cieslar, I. Stulikova, F. Chmelik, and R. K. Islamgaliev, Phys. Status Solidi A **191**, 391 (2002).
12. R. Wuerschum, B. Oberdorfer, E.-M. Steyskal, W. Sprengel, W. Puff, Ph. Pikart, Ch. Hugenschmidt, and R. Pippan, Physica B (Amsterdam) **407**, 2670 (2012).
13. B. Oberdorfer, E.-M. Steyskal, W. Sprengel, and W. Puff, Phys. Rev. Lett. **105**, 146101 (2010).
14. J. Cizek, I. Prochazka, M. Cieslar, R. Kuzel, J. Kuriplach, F. Chmelnik, I. Stulikova, F. Becvar, O. Melikhova, and R. K. Islamgaliev, Phys. Rev. B: Condens. Matter **65**, 094106 (2002).
15. P. V. Kuznetsov, I. V. Petrakova, T. V. Rakhmatulina, A. A. Baturin, and A. V. Korznikov, Zavod. Lab., Diagn. Mater. **78**, 26 (2012).
16. P. V. Kuznetsov, I. V. Petrakova, O. G. Sanarova, and A. V. Korznikov, Deform. Razrushenie Mater., No. 1, 33 (2012).
17. A. V. Korznikov, G. F. Korznikova, M. M. Myshlyaev, R. Z. Valiev, D. Salimonenko, and O. Dimitrov, Phys. Met. Metallogr. **84** (4), 413 (1997).
18. Yu. R. Kolobov, N. V. Girsova, K. V. Ivanov, G. P. Grabovetskaya, and O. B. Perevalova, Russ. Phys. J. **45** (6), 547 (2002).
19. Yu. S. Bordulev, R. S. Laptev, G. V. Garanin, and A. M. Lider, Sovrem. Naukoemkie Tekhnol., No. 8, 184 (2013).
20. Y. S. Bordulev, R. S. Laptev, V. N. Kudiyarov, and A. M. Lider, Adv. Mater. Res. **880**, 93 (2014).
21. R. S. Laptev, Y. S. Bordulev, V. N. Kudiyarov, A. M. Lider, and G. V. Garanin, Adv. Mater. Res. **880**, 134 (2014).
22. D. Giebel and J. Kansy, Phys. Procedia **35**, 122 (2012).
23. D. Giebel and J. Kansy, Mater. Sci. Forum **666**, 138 (2010).
24. *The SP-Program*. http://www.ifj.edu.pl/~mdryzek/page-1ro.htm.
25. S. Mantl and W. Triftshäuser, Phys. Rev. B: Solid State **17**, 1645 (1978).
26. L. Liszkay, C. Corbel, L. Baroux, P. Hautojarvi, M. Bayhan, A. W. Brinkman, and S. Tatarenko, Appl. Phys. Lett. **64**, 1380 (1994).
27. M. J. Puska and R. M. Nieminen, J. Phys. F: Met. Phys. **13**, 333 (1983).
28. G. Dlubek, O. Brummer, N. Meyendorf, P. Hautojarvi, A. Vehanen, and J. Yli-Kauppila, J. Phys. F: Met. Phys. **9**, 1961 (1979).
29. B. L. Shivachev, T. Troev, and T. Yoshiie, J. Nucl. Mater. **306**, 105 (2002).
30. E. V. Kozlov, N. A. Koneva, and N. A. Popova, Fiz. Mezomekh. **12** (4), 93 (2009).
31. Z. Q. Yang, Mater. Lett. **60**, 3846 (2006).
32. M. Alatalo, B. Barbiellini, M. Hakala, H. Kauppinen, T. Korhonen, M. J. Puska, K. Saarinen, P. Hautojarvi, and R. M. Nieminen, Phys. Rev. B: Condens. Matter **54**, 2397 (1996).
33. S. V. Divinski, G. Reglitz, M. Wegner, M. Peterlechner, and G. Wilde, J. Appl. Phys. **115**, 113503 (2014).
34. A. G. Crocker, M. Doneghan, and K. W. Ingle, Philos. Mag. A **41**, 21 (1980).
35. V. I. Betekhtin, E. D. Tabachnikova, A. G. Kadomtsev, M. V. Narykova, and R. Lapovok, Tech. Phys. Lett. **37** (8), 767 (2011).
36. V. I. Betekhtin, A. G. Kadomtsev, V. Skienicka, and I. Saxi, Phys. Solid State **49** (10), 1874 (2007).